Electronic Supplementary Information

Bioinspired Hydrogen Bond Crosslink Strategy toward Toughening Ultrastrong and Multifunctional Nanocomposite Hydrogels

Fengcai Lin,[a] Zi Wang,[a] Jingsi Chen,[c] Beili Lu,[a] Lirong Tang,[a] Xuerong Chen,[a] Chensheng Lin,[b] Biao Huang, *[a] Hongbo Zeng, *[c] Yandan Chen*[a]

[a] College of Material Engineering, Fujian Agriculture and Forestry University, Fuzhou 350108, China.

[b] Fujian Key Laboratory of Developmental and Neural Biology, College of Life Sciences, Fujian Normal University, Fuzhou 350108, China.

[c] Department of Chemical and Materials Engineering, University of Alberta, Edmonton, Alberta, T6G 1H9, Canada.

* Corresponding Author

E-mail: fjaucyd@163.com (Y.C.).

E-mail: hongbo.zeng@ualberta.ca (H.Z.).

E-mail: bhuang@fafu.edu.cn (B.H.).

Experimental

1.1. Materials

Bleached bamboo pulp (α-cellulose content＞95%) was provided by Nanping Paper Co., Ltd. (Nanping, Fujian, China) and beaten to form powdered cellulose with high efficiency pulverize. Poly(vinyl alcohol) (PVA, *DS*=1750 ± 50, M_w=75,000-80,000 g/mol, over 99.0% purity), iron (III) chloride hexahydrate ($FeCl_3 \cdot 6H_2O$, over 99.0% purity), tannic acid (TA, M_w=1701.2, over 99.0% purity) and sulfuric acid (H_2SO_4, over 99.0% purity) were purchased from Sinopharm Chemical Reagent Co., Ltd. (Beijing, China). All the chemicals were used without further purification, and distilled water was used for the preparation of aqueous solutions.

1.2. Preparation of cellulose nanocrystals

Cellulose nanocrystals (CNC) was extracted from bamboo cellulose pulp by acid hydrolysis according to our previous literature.[1] 2.0g of cellulose pulp was hydrolyzed in 100mL sulfuric acid solution (50 wt%) at 65℃ under ultrasonic treatment with vigorous stirring for 60 min. The obtained suspension was several times washed with distilled water by successive centrifugation, and then the CNC suspension was collected through a sequence of repeated centrifugation. The obtained CNC suspension was then dialyzed against distilled water until neutrality and concentrated to 5 wt %. The resultant CNC displayed a short rod-like structure, with a length of 100-300 nm and a diameter of 10-35 nm, as characterized by transmission electron microscopy (TEM) (Fig. S1).

1.3. Hydrogel preparation

Firstly, PVA/CNC hydrogels were prepared, and TA-PVA/CNC hydrogels were constructed. The PVA/CNC hydrogels were prepared by cyclic freeze-thaw process. Typically, PVA powder

and a desired amount of CNC suspension was dissolved in fixed amount of distilled water and then heated to 95℃ with vigorous stirring for 2 h to obtain a homogeneous solution. The final concentration of PVA in solution was set to 10 wt %, and the compositions of CNC were 0 wt %, 5 wt %, 10 wt %, 15 wt %, 20 wt %, 25 wt% with respect to the weight of PVA. After cooling to room temperature, the mixtures were poured into the mold, frozen at -25℃ for 12 h, and subsequently thawed to room temperature over 6 h. This freezing-thawing cycle was repeated 3 times, and then the PVA/CNC hydrogels was obtained. Subsequently, the prepared PVA/CNC hydrogels with thickness of 1.0 mm were soaked in a sufficient amount of TA solution at different concentrations (0 wt %, 5 wt %, 10 wt %, 15 wt %, 20 wt %) for 48 h in dark environment at room temperature to form multiple hydrogen bonding crosslinked hydrogels. The obtained hydrogels were coded as TA*x*-PVA/CNC*y*, where *x* and *y* are the concentration of TA (C_{TA}) and CNC (C_{CNC}), respectively. As a control, the pure PVA hydrogel were also prepared and designated as PVA-gel. The preparation and physiochemical properties of TA-PVA/CNC hydrogels were shown in Scheme 1 and Table S1.

1.4. Water content

The water content (W_{H_2O}) of the hydrogels were calculated using Equation (1).

$$W_{H_2O} = \frac{M_w - M_d}{M_w} \times 100\% \qquad (1)$$

where M_w and M_d are the weights of TA-PVA/CNC hydrogel before and after freeze-drying, respectively.

1.5. Mechanical measurement

A universal material testing machine (Instron 1185, UK) was used to measure the mechanical properties of the hydrogels at room temperature. As for the tensile and loading-unloading tests,

the hydrogels were cut into dumbbell shapes and the stretching rate was 100 mm min^{-1}. In the compression tests, the cylindrical hydrogels with a diameter of 10 mm and a height of 15 mm were set on the lower plate and compressed by the upper plate at a strain rate of 10 mm min^{-1}. The elastic modulus, toughness, and dissipated energy of the samples were calculated from the stress-strain curves with all the test repeated three times.

1.6. Fourier transform infrared (FTIR) and X-ray photoelectron spectroscopy (XPS) analysis

FTIR spectra of the samples in KBr discs were performed on a NICOLET 380 FTIR spectrometer (Thermo Electron Instruments Co., Ltd., USA). The test specimens were carried out in the range of 400-4000 cm^{-1} with 32 scans. X-ray photoelectron spectroscopy (Thermo Electron corporation, USA) was conducted with monochromatic Al Kα radiation (1254.0 eV). Spectra were recorded over a range of 0-1300eV, followed by high resolution scan of the O1s and C1s regions.

1.7. Morphological observation

TEM observations of diluted CNC suspensions were carried out on a Hitachi H-7650 (Japan) electron microscope at an acceleration voltage of 80 kV. The microstructure of the hydrogels was observed by scanning electron microscope (SEM, SU8010, Hitachi, Japan) at an acceleration voltage of 40 kV. Before observation, hydrogel samples were freeze-dried and coated with gold.

1.8. Self-recovery test

The successive loading-unloading tests of hydrogels were also conducted by the above tensile tester, and the stretching rate was fixed at 100 mm min^{-1}. For recovery experiments, the hydrogel samples were first conducted a tensile loading-unloading cycle, and then the samples

were sealed in the plastic dish and stored at room temperature for desired time. Then the samples were taken out for further tests. The 50 continuous compression-relaxation cycles were performed by load-unload mode with a compression velocity of 10 mm min^{-1} and compression strain of 50%. The energy dissipation during each cycle was calculated form the area between the loading-unloading curves. To avoid water evaporation during cyclic test, a thin layer of silicon oil was applied on the hydrogel surface.

1.9. Healing test

The TA15-PVA/CNC20 hydrogel strips (5 cm × 0.5 cm × 0.2 cm) were cut into two halves, and then the cut surfaces were put together without applying any pressure. After adding a droplet of TA solution (15 wt%) or Fe^{3+} solution (0.3 mol/L) on the contact surfaces, the samples were stand for 24 h at room temperature. After healing, the tensile test is carried out again to calculate the healing efficiency (Healing efficiency = $(S-S_0)/S_0$, where S_0 and S are the tensile stress of original and healed hydrogel).

1.10. Adhesion measurement

The adhesive strength of TA-PVA/CNC hydrogels on the various substrate surface was measured by a universal material testing machine (Instron 1185, UK). Fresh porcine skin was cut into 20 mm × 20 mm squares and attached to steel plates (20 mm × 50 mm × 2mm) with cyanoacrylate glue. Then, a TA-PVA/CNC hydrogel with 20 mm × 20 mm × 1mm was placed between two epidermis of porcine skin and compressed with a 100 g weight for 5 min. Next, the adhered plates were pulled to separation at a speed of 10 mm/mim on the universal material testing machine. The adhesion strength was calculated by the measured maximum load divided by the adhesive areas. The different substrate material including glasses, wood, plastic, polytetrafluoroethylene (PTFE), aluminum and stainless steel were also used to investigate the adhesive strength of the hydrogel. All the measurements were performed five times in parallel.

1.11. Cytocompatibility tests

TA-PVA/CNC hydrogels were fabricated into disks of 35 mm diameters and incubated with 75% ethanol, exposed to UV light for 2 h, followed by rinsing with sterile PBS 3 times, then further soaked with cell culture medium (DMEM, supplemented with 10% fetal bovine serum) 3~5 times (3 hours each time) at 37℃ in a humidified 5% CO_2 incubator until the pH of the medium no longer changed. The cytotoxicity of the scaffold was assessed by NIH 3T3 cells labelled with green fluorescent protein (GFP) and the method of in vitro cell culture was performed as described in our previous report.[2] The hydrogels co-cultured with the labelled cells were carefully washed with 37% sterile PBS to remove dead cells, and then fixed with 4% paraformaldehyde solution for 5 minutes. The hydrogels were gingerly placed on a glass slide, sealed with VECTASHIELD Antifade Mounting Medium (Vectorlabs, H-1000) and the coverslip was covered. The images and 3D movie were acquired by a laser scanning confocal microscope (Zeiss, LSM 780) and used to compare the difference in cell number. At least 5 images of each sample were randomly selected for image analysis.

1.12. Antibacterial performance

The antibacterial performance of TA-PVA/CNC hydrogels were evaluated by *Escherichia coli* (*E. coli*) and *Staphylococcus aureus* (*S. aureus*) as Gram-negative and Gram-positive bacteria models via inhibition zone method. The hydrogels were cut into disks with a diameter of 23 mm, and then exposed to UV light for 60 min per side. 100 μL of *E. coli* or *S. aureus* in broth (2×10^4 CFU/mL) was dispersed onto the agar culture medium respectively. Next, the hydrogel disks were carefully placed onto the surface of the agar plate and incubated for 12 h at 37℃. After incubation, the inhibition halos around the samples were observed and their

diameters were measured.

Table S1. Physiochemical properties of TA-PVA/CNC nanocomposite hydrogels

Sample	C_{PVA} (wt%)	C_{CNC} (wt%)	C_{TA} (wt%)	Water content (wt%)
PVA-gel	10	0	0	90.0
TA10-PVA/CNC0	10	0	10	54.08
TA10-PVA/CNC5	10	5	10	51.88
TA10-PVA/CNC10	10	10	10	50.74
TA10-PVA/CNC15	10	15	10	48.01
TA10-PVA/CNC20	10	20	10	45.44
TA10-PVA/CNC25	10	25	10	44.41
TA0-PVA/CNC20	10	20	0	88.0
TA5-PVA/CNC20	10	20	5	62.25
TA10-PVA/CNC20	10	20	10	45.44
TA15-PVA/CNC20	10	20	15	43.35
TA20-PVA/CNC20	10	20	20	42.81

Table S2. Mechanical properties of TA-PVA/CNC nanocomposite hydrogels.

Sample	Tension				Compression			
	σ [MPa]	ε [%]	E [MPa]	U (MJ m^{-3})	σ [MPa]	E [%]	E [MPa]	U (MJ m^{-3})
PVA-gel	0.48	267.74	0.12	0.57	4.73	86.1	0.16	0.51
TA10-PVA/CNC0	2.88	533.76	0.67	7.32	18.60	>90	0.27	1.61
TA10-PVA/CNC5	3.94	711.67	0.80	15.93	26.75	>90	0.42	2.30
TA10-PVA/CNC10	4.63	761.84	0.94	20.03	38.66	>90	0.60	3.25
TA10-PVA/CNC15	6.23	918.81	1.47	31.23	43.21	>90	1.51	3.77
TA10-PVA/CNC20	7.58	1034.31	1.68	42.09	51.62	>90	1.98	4.52
TA10-PVA/CNC25	6.71	842.67	1.42	30.61	54.77	>90	2.13	4.77
TA0-PVA/CNC20	1.56	382.28	0.36	2.82	9.45	>90	0.38	0.77
TA5-PVA/CNC20	4.84	717.83	1.10	18.75	33.93	>90	0.80	2.67
TA10-PVA/CNC20	7.58	1034.31	1.66	42.09	51.61	>90	1.96	4.52
TA15-PVA/CNC20	8.34	1089.57	1.96	50.03	64.66	>90	2.27	5.27
TA20-PVA/CNC20	8.71	1107.55	3.44	58.17	67.90	>90	2.34	6.07

σ, ε, E, and U are the fracture stress, strain at break, elastic modulus, and fracture toughness (calculated from the area under the stress-strain curve).

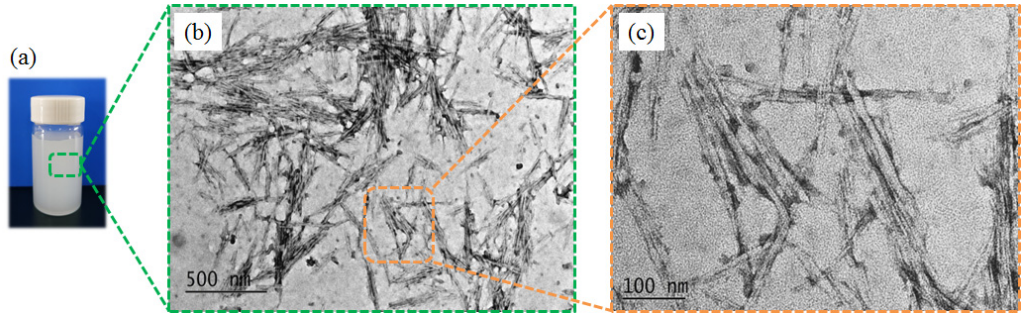

Fig. S1. Physical appearance of CNC suspension (2.0 wt%) (a) and its TEM images (b, c).

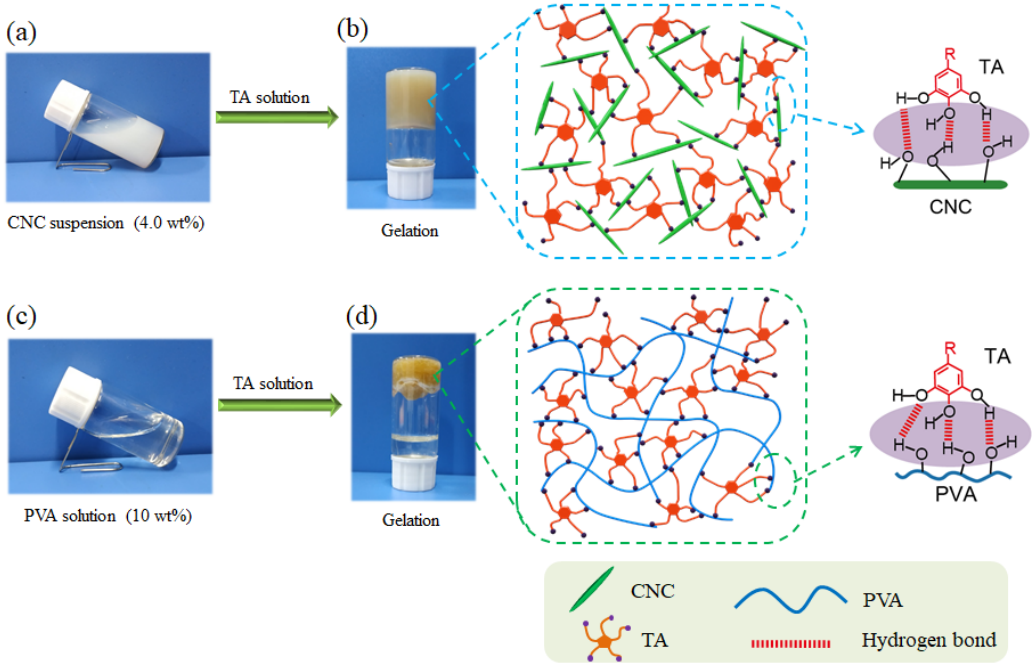

Fig. S2. The gelation behaviors of CNC suspension (a-b) and PVA solution (c-d) after adding TA solution and the possible mechanism of formation via multiple hydrogen bonding.

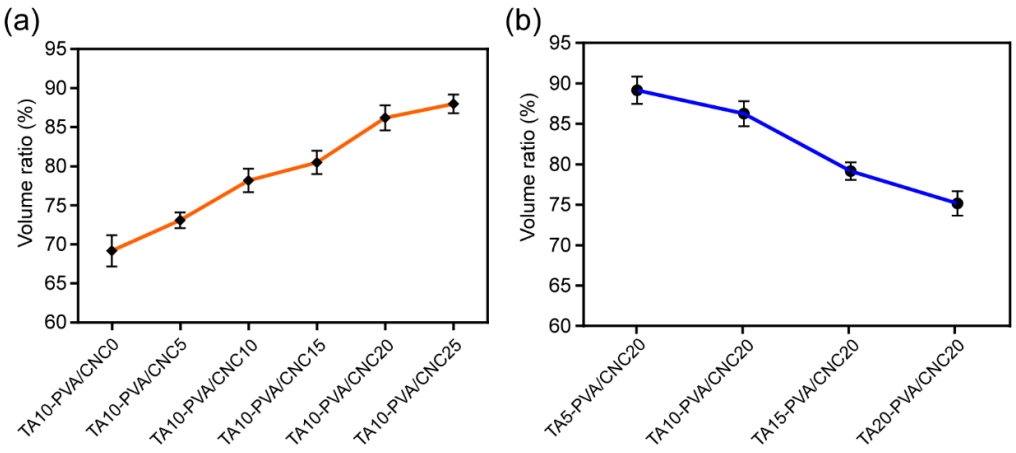

Fig. S3. Volume ratio of TA-PVA/CNC hydrogels to PVA/CNC hydrogel: (a) TA10-PVA/CNC*x* hydrogels (C_{TA} = 10 wt%) with different CNC mass concentration (*x*= 0, 5, 10, 15, 20, 25wt%); (b) TA*y*-PVA/CNC20 hydrogels (C_{CNC} = 20 wt%) by different TA fraction (*y*=5, 10, 15, 20wt%) treatment. The volume ratio of TA-PVA/CNC hydrogel to PVA/CNC hydrogel increased with the increase of C_{CNC}, indicating that the stiff CNC participated in the structural construction of TA-PVA/CNC hydrogels. On the other hand, the volume ratio decreased with increas of C_{TA}, which was attributed to the intensive H-bond interactions between TA and PVA/CNC matrix that significantly made the interchain close to obtain TA-PVA/CNC hydrogel with much denser microstructure.

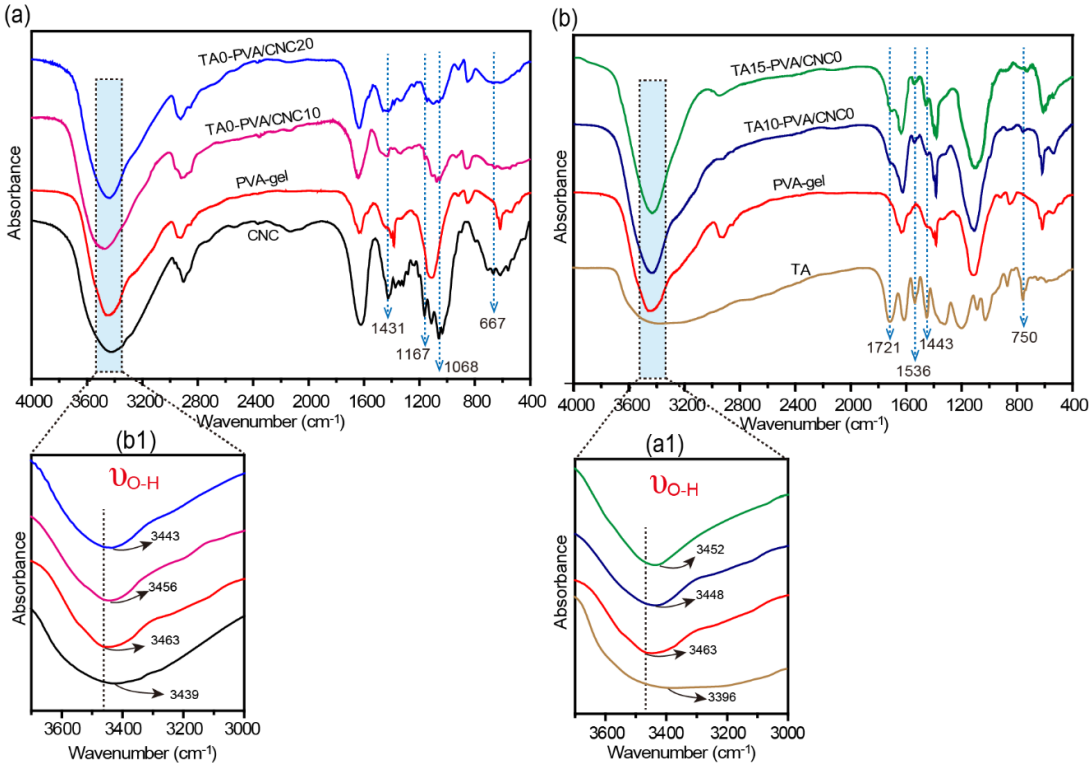

Fig. S4. (a) FTIR spectra of CNC, PVA-gel, and TA0-PVA/CNC hydrogels. (b) FTIR spectra of TA, PVA-gel, and TA-PVA/CNC0 hydrogels.

Fig. S4 showed the FTIR spectra of the CNC, TA, PVA-gel, TA0-PVA/CNC (PVA hydrogel with different CNC content), and TA-PVA/CNC0 (PVA hydrogel treated with different concentration of TA solution) hydrogels. As displayed in Fig. S4a, after introducing the CNC into PVA-gel, the specific peaks of PVA were relatively well retained and some notable stretching peaks at 1431 cm^{-1} ($-CH_2$ stretching vibration), 1167 cm^{-1} (C-O-C symmetrical stretching vibration), 1068 cm^{-1} (C-O stretching vibration), and 667 cm^{-1} (C-H asymmetric stretching vibration) appeared, suggesting the presence of CNC in TA0-PVA/CNC hydrogels.[3] For PVA-gel, the stretching vibration of -OH groups at 3463 cm^{-1} displayed a strong absorption peak, arising from the H-bonding interactions in PVA-gel (Fig. S4a1). For TA0-PVA/CNC10 and TA0-PVA/CNC20, this absorption peak gradually shifted to lower wavenumber at 3456 cm^{-1} and 3443 cm^{-1} with the increment of CNC contents in the PVA-gel,

confirming the presence of H-bonding interactions between the PVA and CNC.[4] Similarly, as shown in Fig. S4b, after treating PVA-gel with TA, the peak assigned to C=O, aromatic C-C, phenolic hydroxyl of TA was appeared at 1721 cm^{-1}, 1536 cm^{-1}, 1443 cm^{-1}, and 750 cm^{-1} in the spectrum of TA10-PVA/CNC0 and TA15-PVA/CNC0. Due to the H-bonding interactions between the PVA and TA, the stretching vibration of -OH groups at 3463 cm^{-1} for PVA-gel were shifted to 3448 cm^{-1} and 3452 cm^{-1} for TA10-PVA/CNC0 and TA15-PVA/CNC0 with the increment of TA content (Fig. S4b1).[5-7]

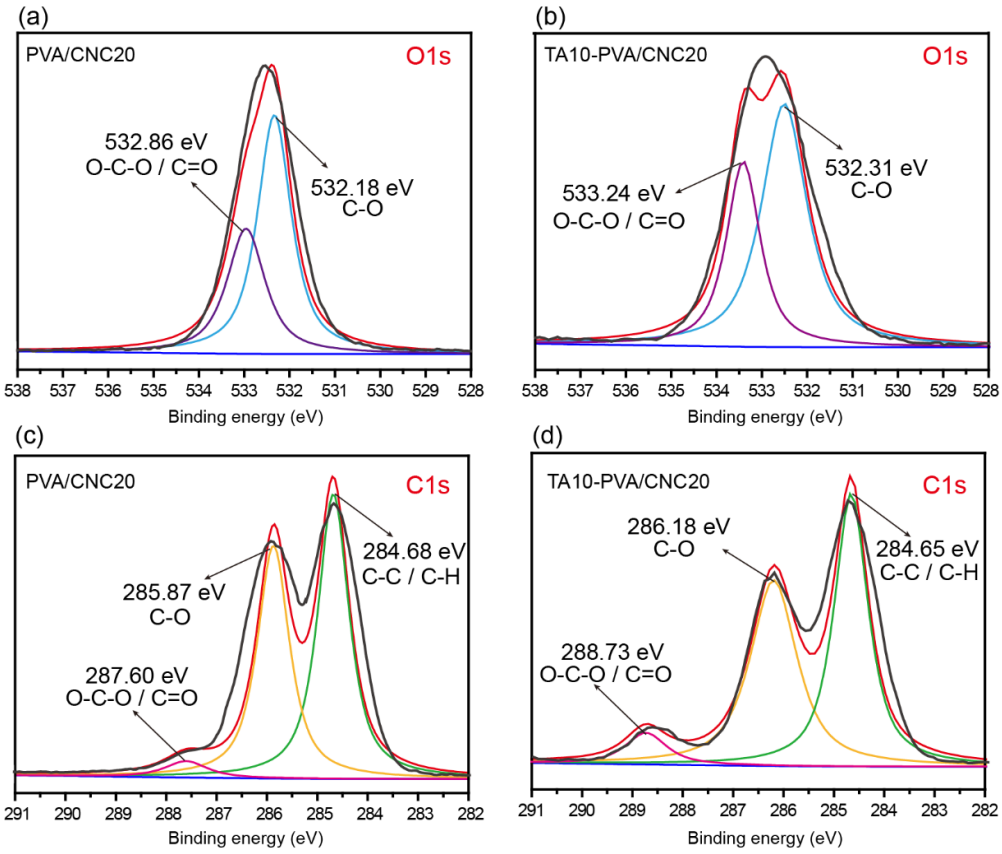

Fig. S5. O1s XPS spectra of TA0-PVA/CNC20 (a) and TA10-PVA/CNC20 (b). C1s XPS spectra of TA0-PVA/CNC20 (c) and TA10-PVA/CNC20 (d).

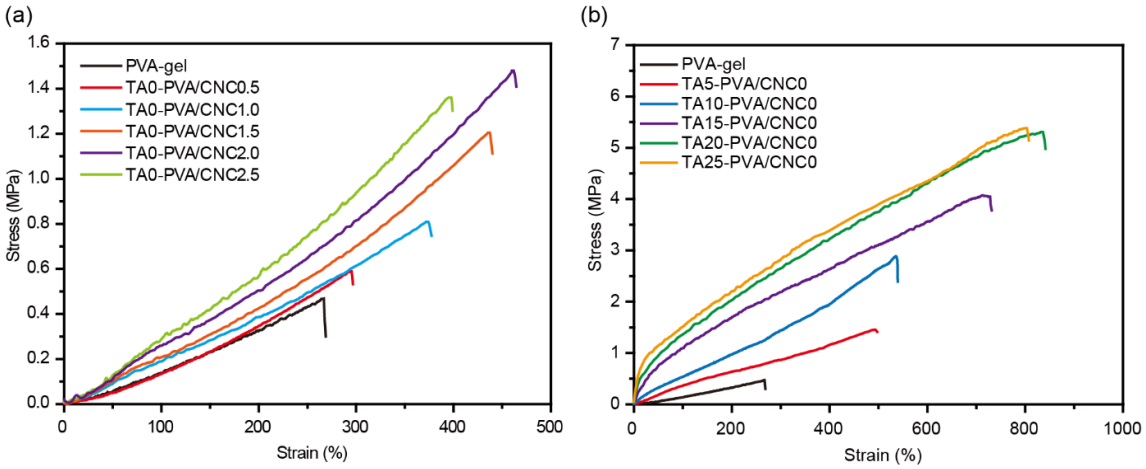

Fig S6. (a) Typical tensile stress-strain curves of the TA0-PVA/CNC hydrogels (PVA hydrogel with different CNC content). (b) Typical tensile stress-strain curves of the TA-PVA/CNC0 hydrogels (PVA hydrogel treated with different concentration of TA solution).

Fig. S6a illustrates the effects of the CNC content on the tensile strength of PVA-CNC hydrogels. It was clearly shown that the mechanical strength of nanocomposite hydrogels was obviously higher than that of pure PVA hydrogel. With the increase of CNC content, their tensile stress and strain raised observably and then slightly declined. When the CNC content was 20 wt%, the largest strain reached 461.1 %, while the highest strength reached 1.48 MPa at the same point. These mechanical improvements can be ascribed to the high strength and stiffness of the CNC nanoparticles. Moreover, both PVA and CNC are hydrophilic, so the dispersion and distribution of the CNC in the PVA matrix are uniform, resulting in strong combination between them due to the presence of H-bonding interactions as we previously discussed in FTIR analysis. Fig. S6b shows the tensile stress-strain curves of the TA-PVA hydrogels after treating with different TA mass concentration. Similarly, all mechanical properties of TA-PVA hydrogels increased with increasing TA concentration until 15 wt% and then kept constant. This significantly improved mechanical strength was attributed to the strong H-bonding interactions between TA and PVA chains, which has been well validated in previous work[5-7] and our above

FTIR analysis.

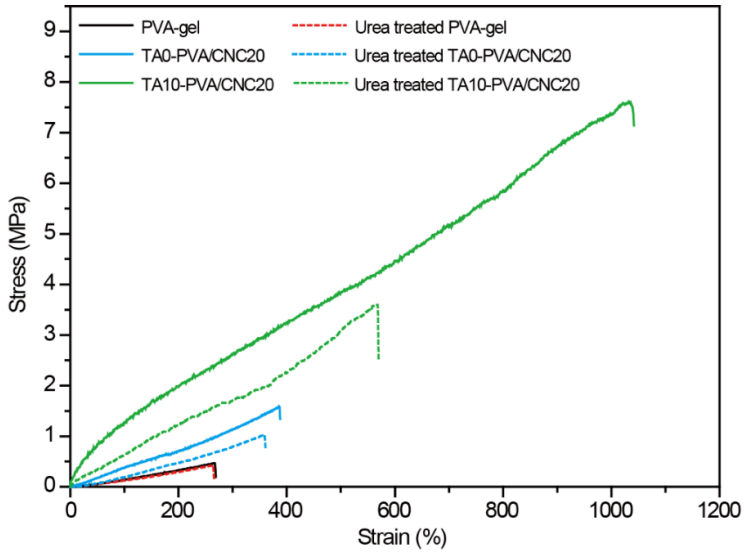

Fig. S7. Effect of urea treatments on the mechanical properties of the PVA-gel, TA0-PVA/CNC20 and TA10-PVA/CNC20 hydrogel.

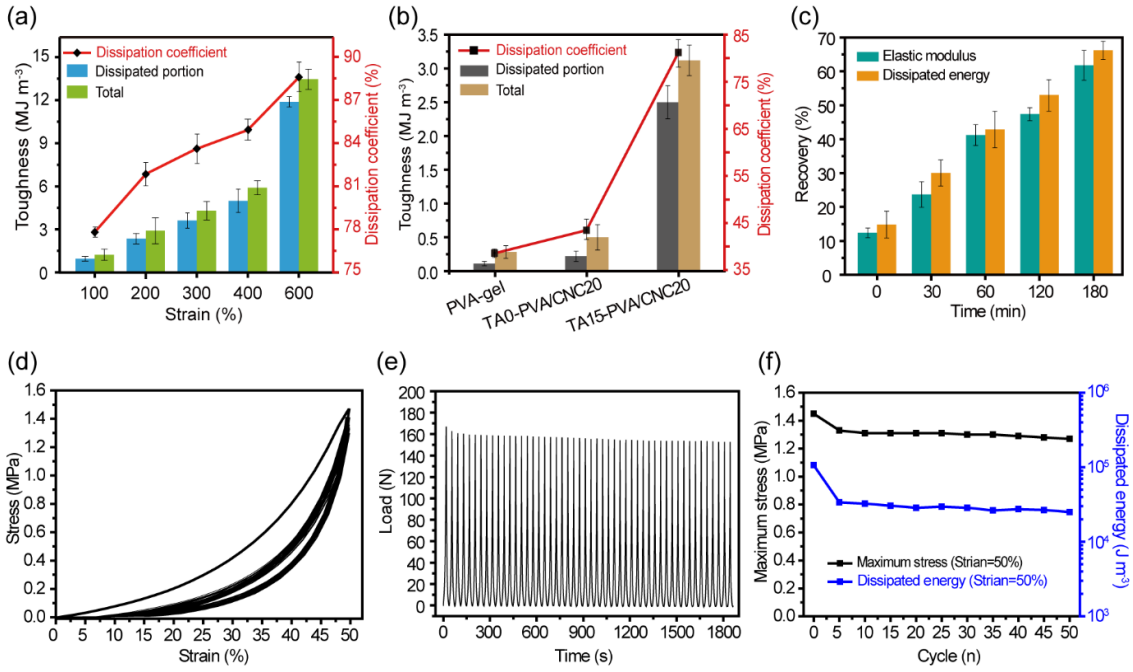

Fig. S8. (a-b) The total energy, dissipated energy and energy dissipation coefficient of samples calculated from Fig. 4a and Fig. 4d, respectively. (c) The time dependence recovery of elastic

modulus and hysteresis loop of TA15-PVA/CNC20 calculated from Fig. 4c. (d) The stress-strain curve and (e) load-time curve of fifty successive compression-relaxation cycles of TA15-PVA/CNC20 hydrogel. (f) The maximal stress and dissipated energy of TA15-PVA/CNC20 hydrogels every five cycles in 50 continuous compression-relaxation cycles.

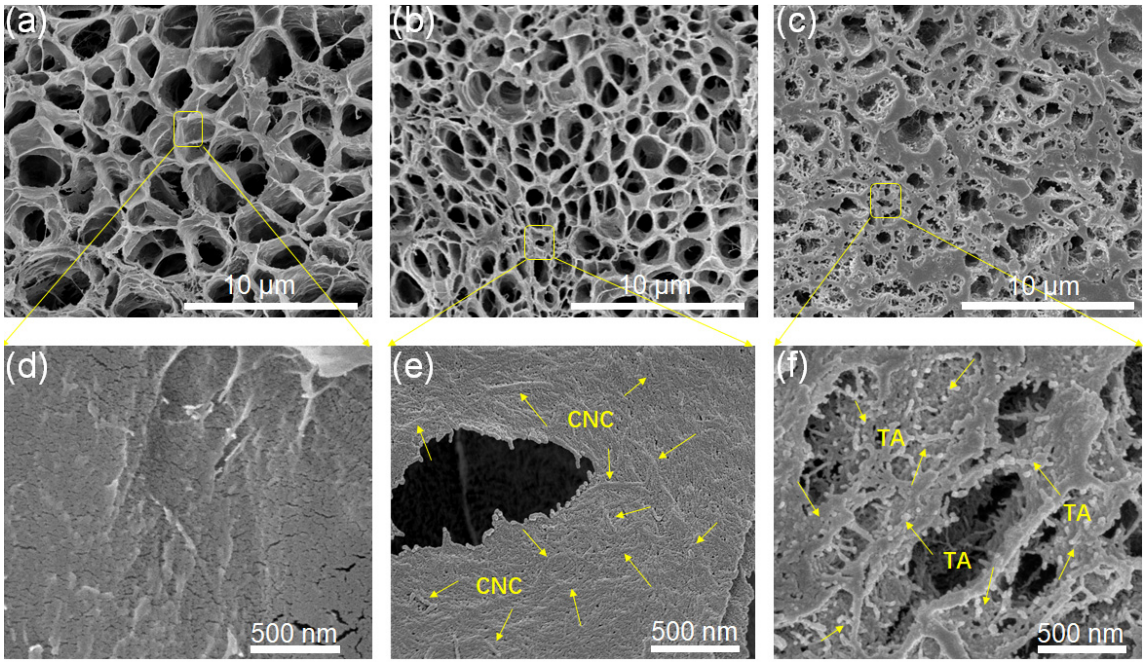

Fig. S9. SEM image of PVA-gel (a, d), TA0-PVA/CNC20 (b, e), and TA15-PVA/CNC20 (c, f) hydrogels.

References

1. Q. Lu, L. Tang, S. Wang, B. Huang, Y. Chen and X. Chen, *Biomass Bioenergy*, 2014, **70**, 267-272.
2. F. Lin, R. Zheng, J. Chen, W. Su, B. Dong, C. Lin, B. Huang and B. Lu, *Carbohydr. polym.*, 2019, **205**, 244-254.
3. Q. Lu, L. Tang, F. Lin, S. Wang, Y. Chen, X. Chen and B. Huang, *Cellulose*, 2014, **21**, 3497-3506.
4. Z. Xu and J. Li, *J. Nanosci. Nanotechnol.*, 2018, **18**, 668-675.
5. Y. Chen, L. Peng, T. Liu, Y. Wang, S. Shi and H. Wang, *ACS Appl. Mater. Interfaces,* 2016, **8**, 27199-27206.
6. Y. Chen, C. Jiao, Y. Zhao, J. Zhang and H. Wang, *ACS Omega*, 2018, **3**, 11788-11795.
7. R. Xu, S. Ma, P. Lin, B. Yu, F. Zhou and W. Liu, *ACS Appl. Mater. Interfaces,* 2017, **10**, 7593-7601.